AGU PUBLICATIONS

Geochemistry, Geophysics, Geosystems

RESEARCH ARTICLE
10.1002/2017GC007149

Key Points:
- Test of combinations of rotation/growth/superrotation to explain observations of uppermost inner core
- We propagate rays through the models, using random and real distribution with Python tool GrowYourIC
- Slow translation/superrotation is the only model that explain the shift in hemisphere boundaries with depth

Supporting Information:
- Supporting Information S1

Correspondence to:
M. Lasbleis,
marine.lasbleis@elsi.jp

Citation:
Lasbleis, M., Waszek, L., & Day, E. A. (2017). GrowYourIC: A step toward a coherent model of the Earth's inner core seismic structure. *Geochemistry, Geophysics, Geosystems*, *18*, 4016–4026. https://doi.org/10.1002/2017GC007149

Received 19 JUL 2017
Accepted 13 OCT 2017
Accepted article online 20 OCT 2017
Published online 16 NOV 2017

GrowYourIC: A Step Toward a Coherent Model of the Earth's Inner Core Seismic Structure

Marine Lasbleis[1], Lauren Waszek[2,3,4], and Elizabeth A. Day[4,5]

[1]Earth-Life Science Institute, Tokyo Institute of Technology, Meguro, Tokyo, Japan, [2]Department of Physics, New Mexico State University, Las Cruces, NM, USA, [3]Research School of Earth Sciences, Australian National University, Acton, ACT, Australia, [4]Bullard Laboratories, University of Cambridge, Cambridge, UK, [5]Department of Earth Science and Engineering, Imperial College London, South Kensington, UK

Abstract A complex inner core structure has been well established from seismic studies, showing radial and lateral heterogeneities at various length scales. Yet no geodynamic model is able to explain all the features observed. One of the main limits for this is the lack of tools to compare seismic observations and numerical models successfully. We use here a new Python tool called GrowYourIC to compare models of inner core structure. We calculate properties of geodynamic models of the inner core along seismic raypaths, for random or user-specified data sets. We test kinematic models which simulate fast lateral translation, superrotation, and differential growth. We explore first the influence on a real inner core data set, which has a sparse coverage of the inner core boundary. Such a data set is however able to successfully constrain the hemispherical boundaries due to a good sampling of latitudes. Combining translation and rotation could explain some of the features of the boundaries separating the inner core hemispheres. The depth shift of the boundaries, observed by some authors, seems unlikely to be modeled by a fast translation but could be produced by slow translation associated with superrotation.

Plain Language Summary The Earth's inner core is the solid part of the Earth's core located at the very center of the Earth. It is slowly crystallizing from the liquid outer core, powering the geodynamo and generating the magnetic field. The inner core's structure, detected via observations of seismic waves, is complex and still not elucidated. No model has yet been successful at explaining its different features, and questions as simple as when did the inner core started crystallizing are still unanswered.In this work, we propose a new framework to study seismic properties of the inner core, combining models of how materials flow and seismic data set. We developed an open-access and easy-to-use software to compare both predictions and real data. This toolbox will help us understand what is happening at the very center of our planet, and rule out proposed models. By understanding the inner core dynamics, we hope to better comprehend the thermal and compositional history of the deepest parts of our planet.

1. Introduction

At Earth's center, the inner core is a distant and enigmatic region, yet has wide ranging effects. The inner core grows over time, releasing heat and light elements which help to drive convection in the outer core, with implications for the geodynamo and heat transport to the mantle (Labrosse, 2003). Recent detailed seismic studies have greatly enhanced our understanding of the seismic velocity and attenuation properties in the inner core. However, these observations cannot be recreated by current geodynamic models, nor reconciled with results from mineral physics. This is especially problematic for understanding the origins of the structures: are they a frozen remnant of the early thermal history of the Earth, or an indication of today's flow in the inner core?

The inner core displays large-scale variations in its seismic properties. The major feature is an apparent anisotropy in seismic velocity and attenuation, coupled with a hemispherical dichotomy. Anisotropy in seismic velocity and attenuation is aligned to the Earth's rotation axis, with polar paths displaying higher velocity and stronger attenuation (Morelli et al., 1986; Poupinet et al., 1983; Woodhouse et al., 1986). The inner core is separated into distinct hemispheres, approximately east and west, with regional variation superimpose (Cao & Romanowicz, 2004; Cormier et al., 2011; Creager, 1992; Niu & Wen, 2001, 2002; Tanaka & Hamaguchi, 1997;

Yu & Wen, 2007). The west hemisphere has lower seismic velocity, weaker attenuation, and stronger anisotropy. The anisotropy increases with depth (Deuss et al., 2010; Irving & Deuss, 2011a), and the upper west hemisphere has complicated layering including a isotropic upper layer of 50–100 km thickness (Ouzounis & Creager, 2001; Shearer, 1994; Song & Helmberger, 1995; Waszek & Deuss, 2011). These hemispheres are detected almost to the center of the core (Lythgoe et al., 2014). Improved resolution from expanding seismic data sets has revealed increasingly complex features, such as sharp boundaries separating the hemispheres (Waszek & Deuss, 2011), which may shift with depth in the inner core or laterally (Irving, 2016; Irving & Deuss, 2015; Miller et al., 2013; Waszek et al., 2011).

Two mechanisms have been proposed to generate the seismic hemispheres, driven by either inner core or outer core flow. The first mechanism invokes a lateral translation of the inner core driven by a thermal convective instability. The translation generates an asymmetry in age between a solidifying hemisphere and a melting one. To fit seismic observations, an eastward translation has been proposed, the melting occurring on the east side of the inner core (Alboussière et al., 2010; Monnereau et al., 2010). The translation velocity is estimated $\approx 4\times10^{-10}$ m s^{-1}, corresponding to a complete renewal of inner core material on timescales of $\approx$200 Myr. In this model, age is correlated to crystal size, with larger crystals—or domain size—in older material (Bergman et al., 2010), and thus with seismic velocity and attenuation properties (Calvet & Margerin, 2008). Since the translation is driven by the inner core, any superrotation of the inner core may also rotate the translation axis. This is a problem for the seismically proposed inner core superrotation (Song & Richards, 1996; Vidale & Earle, 2000; Waszek et al., 2011).

The second model to generate the hemispheres proposes thermochemical coupling of the inner core to the core-mantle boundary. Variations in heat loss to the mantle cause faster solidification in the east hemisphere (Aubert et al., 2008, 2013). The resultant difference in growth rate creates smaller crystals in the east hemisphere than the west, generating the seismic observations. The difference in crystal size is therefore opposite to the structure which would arise from lateral translation. Here the process to create differential growth may also produce extremely slow inner core superrotation (Aubert & Dumberry, 2011).

It is beyond the scope of these geodynamic models to explain seismic structures more complex than an east-west asymmetry. Neither mechanism can generate a global depth-dependent velocity anisotropy (Creager, 2000; Irving & Deuss, 2011b; Shearer, 1994; Song & Helmberger, 1995; Waszek & Deuss, 2011), nor attenuation anisotropy (Souriau, 2009; Souriau & Romanowicz, 1996). Recent observations of latitudinal and depth variation in the sharp hemisphere boundaries also reveal more complexity than may be incorporated in the models (Irving, 2016; Irving & Deuss, 2015; Miller et al., 2013; Waszek & Deuss, 2011).

It is important to note that the translation instability is a convective instability, requiring an unstable density profile in the inner core. Lasbleis and Deguen (2015) showed that such a thermal instability is incompatible with some of the other deformation processes usually cited for obtaining the observed anisotropy, such as the differential growth rate at the equator (Deguen et al., 2011; Lincot et al., 2015; Yoshida et al., 1996). Translation may be driven compositionally rather than thermally (Deguen et al., 2013; Gubbins et al., 2013). However, deformation mechanisms to explain the elastic anisotropy require lower viscosity of the inner core than needed by translation, as viscous adjustment would be more efficient and plume convection is predicted in this case (Deguen et al., 2013; Lythgoe et al., 2015; Mizzon & Monnereau, 2013).

In order to understand the origin of the inner core structures, it is imperative to test geodynamic models against seismological observations. Here we present the results obtained with a newly available open-source Python tool GrowYourIC, which aims to recreate inner core seismic structures via a geodynamic modeling approach. Following Monnereau et al. (2010) and Geballe et al. (2013), we focus on processes without shear deformation: growth, translation, and superrotation of the inner core. GrowYourIC utilizes a combination of these geodynamic processes to generate a synthetic inner core. We calculate age and growth rate models for this inner core, then average the values along inner core seismic raypaths. These paths may be random, user specified, or the example data set provided (Waszek & Deuss, 2011; WD11). In this work, we test the hypothesis proposed in (Waszek & Deuss, 2011) that the observed depth variation of the hemisphere boundaries are due to superrotation of the inner core. To do so, we benchmark the tool by revisiting the fast translation model (without growth) of Geballe et al. (2013; GE13) with the real seismic data set (WD11).

This is the first work to test directly the influence of a combination of inner core growth, translation, and superrotation, specifically applied to seismic properties. The reader is invited to download and explore the code in order to reproduce our work, and expand on it by adding functions to produce further complexities.

2. Methods

2.1. Overview of GrowYourIC

The open-source Python tool GrowYourIC computes synthetic seismic properties from geodynamic models, permitting better comparison between observations and geodynamic parameters using realistic seismic data sets. The code is highly modular, allowing the user to easily define new classes for geodynamic models or seismic data sets, with straightforward plotting of results. Jupyter Notebooks (Kluyver et al., 2016) are provided with examples for users to experiment on the code without advanced Python skills, and reproduce all the figures in this paper. Code operations and details about the included models and proxies are available in Appendix A.

Here we model processes that do not have deformation, specifically perfect translation, and superrotation of the translation axis. The models are kinematically parametrized. The flows in the inner core are imposed by setting the velocity in the sphere, as a function $\mathbf{v}(\mathbf{r}, t)$. Translation velocity is estimated from Alboussière et al. (2010), which solves the conservation equations for the end-member case of very fast phase change at the inner core boundary. In this end-member, the vorticity of the flow is zero and no deformation can develop (Deguen et al., 2013). Inner core growth is included by varying the position of the inner core boundary with time. The evolution parameters within the code are extremely flexible, allowing time and spatial variation of velocities, and diverse scenarios of growth. Since anisotropy is primarily negligible in the top 100 km of the inner core (i.e., for the WD11 data used here; Garcia & Souriau, 2000; Ouzounis & Creager, 2001; Song & Xu, 2002; Yu & Wen, 2007), we do not consider crystal anisotropy.

2.2. Proxies and Seismic Observations

The relationship between seismic properties (compressional and shear wave velocities, attenuation, and anisotropy) and outputs of a geodynamic model is not trivial. Elastic properties for iron at high pressure and high temperature are still highly debated (Geballe et al., 2013; Lincot et al., 2014, 2015, 2016), and Lincot et al. (2016) show that the best approach may therefore be to consider mapping of the parameter space. Geballe et al. (2013) explored the relationship between age of material and estimated seismic velocities, based on different crystal growth models, and models of elastic properties for iron crystal clusters. The authors calculated compressional wave velocity as a monotonic function of age alone; i.e., $V_p = f(age)$. This relationship may be generalized by considering seismic properties as a function of various proxies, including age of material (Geballe et al., 2013), crystal growth rate, and crystal orientation (Lincot et al., 2014, 2016); giving $V_p = f(\{proxy_i\}_i)$.

In this study, we refrain from calculating seismic velocities for the different inner core models. Instead, we define the proxies which seek to match the general trends of the seismic observations. This means that we cannot model the observations completely; for example, amplitude of variations, scatter or attenuation. However, our approach also prevents the introduction of additional uncertainties, via poorly constrained assumptions relating age to seismic properties. Without this limitation, rapid exploration of a large range of model parameters and proxies is possible. More complex functions may more closely match the behavior of iron in the inner core. This could account for some of the complexity observed in real seismic data which is beyond the scope of this paper.

2.3. Models

We consider a combination of translation, superrotation, and growth of the inner core. The four different models studied in this paper are presented in Figure 1a, showing flow lines in black solid lines, and age of material as color. The translation is defined as a pure translation along the axis of translation, defined by its vector $\mathbf{e}_T$ and the amplitude of the velocity v_t. The superrotation is defined as a pure rotation around the vertical axis $\mathbf{e}_z$ of amplitude Ω. The corresponding velocity field in the sphere is then $\mathbf{v} = v_t \mathbf{e}_T + \Omega \mathbf{e}_z \times \mathbf{r}$, where $\mathbf{r}$ is the position vector. Trajectory of a given particle in the sphere is calculated by integrating backward in time the velocity, using a fourth-order Runge-Kutta integration scheme. The intersection between

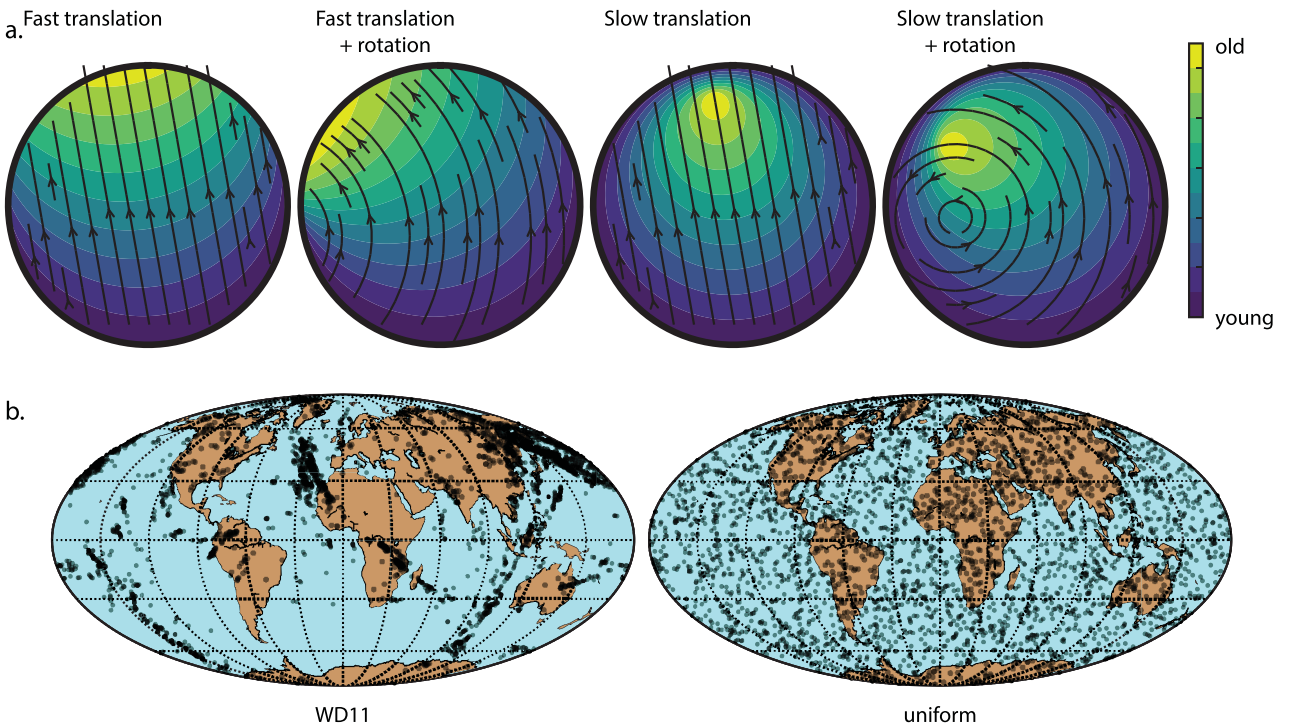

Figure 1. (a) Visualization of the different models used in the paper, with the associated names: fast translation, fast translation associated with superrotation, slow translation, and slow translation associated with superrotation. Details of the values used are available in the supporting information. (b) Horizontal distribution of the two different data sets used in this paper: WD11 (3,184 points) and uniform (3,000 points). The points have a 50% transparency, meaning that they appear grey except when at least two points are overlaid. This highlights the areas of over sampling in WD11.

the trajectory and the inner core boundary defines the position and time of the crystallization of the particle. To model the growth of the inner core, the position $r_{icb}(t)$ of the sphere surface is estimated by a power function $r_{icb}(t)=t^{\alpha}$. For reasonable core thermal and composition thermal history, it is usually considered that α is between 1/3 and 1/2 (Labrosse, 2003). The parameters used in this study for the four different models are given in the supporting information.

Geballe et al. (2013) used a similar approach to calculate the age model for a simple version of the translation but calculated the intersection between straight trajectories and the sphere boundary analytically. The main difference here is that, allowing for superrotation and growth of the inner core, we cannot calculates the intersection analytically.

In this work, the proxies of interest are the age of material, obtained from the time of crystallization, and the growth rate at the time and position of the crystallization. The effective growth rate is calculated by subtracting the velocity to the average growth rate at the time of the crystallization.

2.4. Seismic Databases

In this paper, we present the results for two different seismic data sets. The first is a random distribution of PKIKP turning points, distributed uniformly in the uppermost part of the inner core (depth between 7 and 100 km). The second is the WD11 data set (Waszek & Deuss, 2011), which contains 3184 PKIKP raypaths, defined by their entry, turning, and exit points. Residuals (with respect to the corresponding PKiKP arrival) associated with each raypath are also provided, from tabulated values in Waszek and Deuss (2011). The global distributions of each data set are shown on Figure 1b. The WD11 appears sparse, and oversamples parts of the inner core. This is due to the nonuniform distribution of both seismic events and seismic stations.

Geballe et al. (2013) and Lincot et al. (2015) have previously combined seismic observations and geodynamical models, propagating raypaths into hypothetical seismic raypaths. However, both studies used a random raypath distribution inside the inner core, overestimating the capability of the seismic data to distinguish

between models. In this paper, we use both random and real data sets; both of which are made available online.

We consider whether a simple geodynamic model is able to match any of the detailed seismic observations in WD11. We focus on two main observations: the sharp, and shifting, hemisphere boundaries. As seen in Figure 1b, the data coverage in WD11 is likely to be sufficient to characterize some of the detailed features, and relate them to our models. However, the boundary locations are not well sampled by WD11. Very few data constrain the exact boundary locations; additional data could drastically alter their positions. Despite this, the jump in seismic properties between hemispheres can be restricted to occur over length scales on the order of ~500 km, which is comparatively sharp. Several other studies also find that the Pacific boundary (longitude 160°–180°) is sharper than the African (longitude 20°–60°; Irving, 2016; Irving & Deuss, 2015; Yu & Wen, 2007).

For the remainder of this paper, we will seek to match the proposed sharpness and shift in depth of the boundaries. However, it is important to note that this shifting structure is poorly constrained by the existing data set. Alternative geometries (e.g., latitudinal variation of the boundary locations) are beginning to be revealed by improved seismic data coverage, and should be considered for future models (Irving, 2016; Miller et al., 2013).

3. Discussion

3.1. Fast Translation: Random Versus Real Data Sets

A major question addresses the validity of a random distribution of data to compare with a real seismic data set for use in observations. In other words, is seismic structure of the top of the inner core sampled well enough that the signature of translation could be detected? To explore this, we first compare our results to GE13 (i.e., fast translation only), to explore the efficacy of a random perfect inner core data set versus real data.

Figure 2 recreates GE13 with GrowYourIC, using a random data set sampling the upper layer of the inner core. We find spatial distribution is well matched, with random rays over the full surface of the inner core, and turning depths varying from 15 to 107 km. We calculate the age of material at the turning point, and project it as function of the longitude and angular distance with respect to (0, 100°E), the center of translation in the east hemisphere. Maximum age is obtained as $2R_{ic}/v_t$, with R_{ic} the radius of the inner core and v_t the translation velocity. Our results are equivalent (Figures 2a–2c), validating our method. Unlike

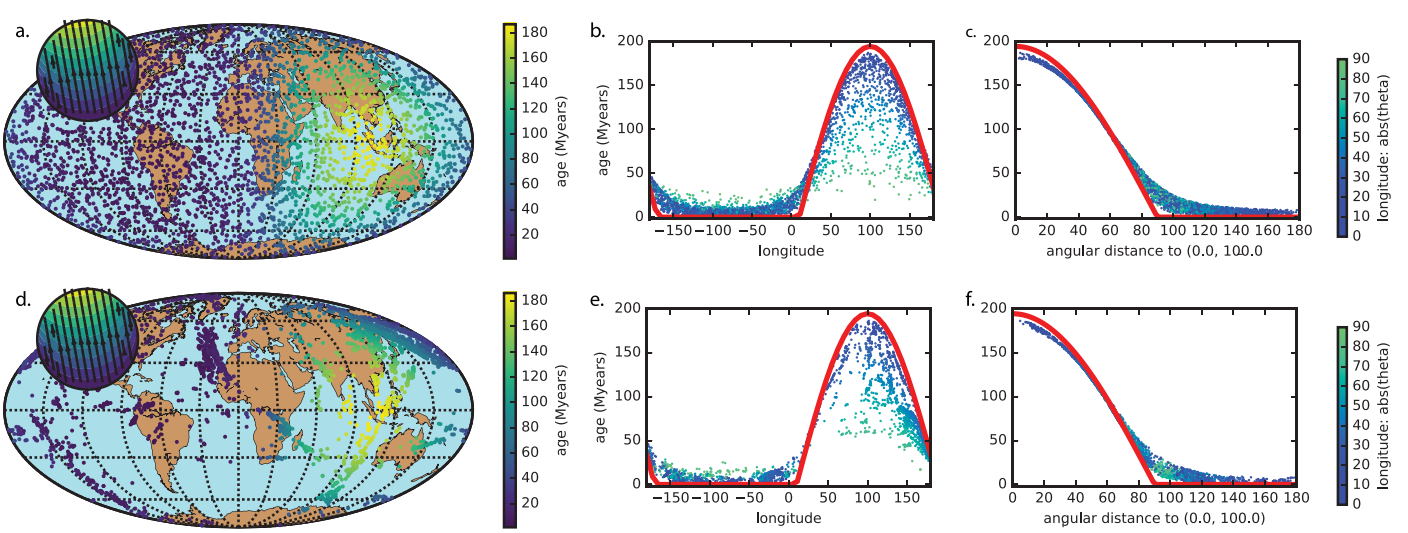

Figure 2. Fast translation as observed by (a–c) random distribution and (d–f) WD11 data set. (a, d) Spatial distribution of the data set. The value of age as function of (b, e) longitude and (c, d) angular distance from the point (0, −80). Red lines correspond to the analytical solution on the equator at the inner core boundary and without growth. Discrepancy between the values of the data and analytical solution comes from the depth and latitude of the point, as well as the inclusion of (slow) growth rate in the example.

Geballe et al. (2013), here we do not calculate theoretical travel time residuals, and instead consider age is a proxy for seismic properties. We assume a monotonic function f, whereby $v_p = f(age)$. For benchmarking the tool GrowYourIC, we also computed the travel time residuals, and results are available in a Jupyter Notebook online.

To estimate the validity of a random distribution, we recalculate the model using a real seismic distribution. We use WD11, which samples the upper 100 km of the inner core. On a map, the distribution is uneven, with clusters in the northern hemisphere, as seen in Figure 1b. However, the translation has a cylindrical symmetry, and the variable of interest is distance from (0, 100°E). The coverage in angular distance from (0, 100°E) is good, except for the highest values, corresponding to the south-east Pacific ocean. Figure 2 thus indicates that this spatial sampling should be adequate to characterize translation, and estimate large-scale features with cylindrical symmetry, such as hemispherical dichotomy.

The hemisphere centers are assumed to be located on the equator, which leads to difficulty using the longitude to estimate the *distance to center* for inner core points away from the equator. This can be seen when we plot data as function of longitude and depth. This geometry was used in Waszek et al. (2011, Figure 2) for example, and is reproduced here in Figure 3, middle and bottom. When including points away from the equator, a scatter appears, that may lead to problem in the interpretation of such a plot. For this reason, we are also plotting data only at the equator, maximizing the observability of the structure, as shown on Figure 3, top.

As discussed before by Geballe et al. (2013) and shown in Figure 2, the sharpness of the hemisphere can be explained by a fast translation. It was then hypothesized by Waszek et al. (2011) that depth variation in the hemisphere boundaries may be indicative of a slow superrotation of the inner core. We therefore investigate the influence of superrotation on the boundary positions with depth, using a rate of 0.09°/Myr, similar to that proposed by Waszek et al. (2011) and Aubert et al. (2008). The contour plot is shown in Figure 3 (top right). No shifting of the boundaries materializes in the upper 100 km. Instead, superrotation induces an asymmetry in the sizes of the hemisphere, producing a larger west hemisphere. The sharpness of the boundaries is also affected by rotation: the Pacific boundary becomes sharper than the African boundary, as superrotation pushes material toward the east. Interestingly, both of these features are observed seismically in WD11, as well as other studies (e.g., Irving, 2016; Irving & Deuss, 2015; Yu & Wen, 2007).

Thus, we find fast translation plus rotation is able to explain some of the more robust seismic observations, namely the sharpness of the different hemisphere boundaries. However, superrotation of the inner core would not be sufficient to explain the depth variation of the boundaries.

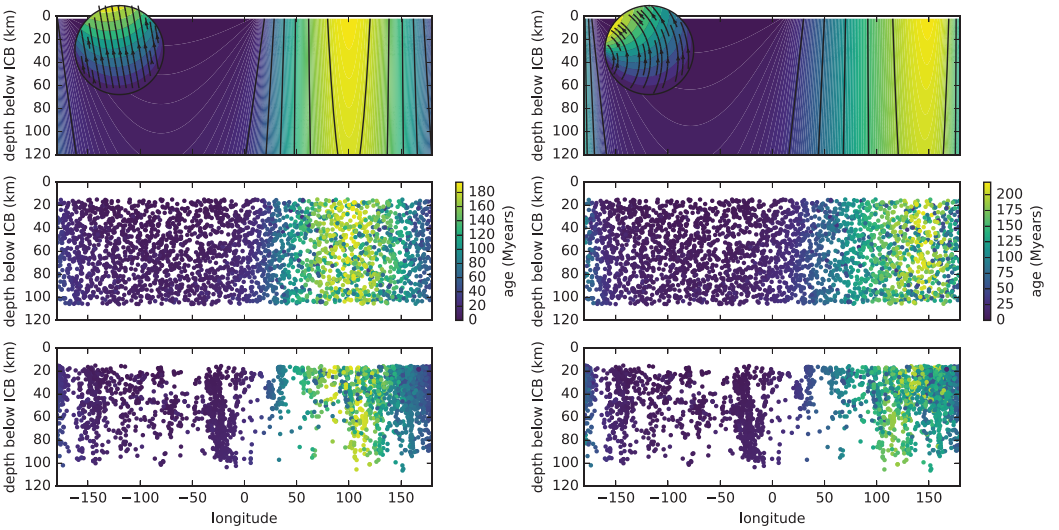

Figure 3. Value of the proxy (age) as a function of the longitude and depth of the observation, for the fast translation model with different data sets, (left column) without and (right column) with superrotation. (top) Contour maps are taken at the equator, and turning depths are from (middle) random global data sets and (bottom) WD11. The scatter in middle and bottom reflect the latitudinal variation. The introduction of superrotation generates an asymmetry in both hemisphere size and boundary sharpness, but no apparent shift in the boundaries with depth.

3.2. Slow Translation: Growth Rate as a Proxy

Aubert et al. (2008) proposed that the thermochemical circulation in the liquid outer core may induce an asymmetry in the growth rate at the surface of the inner core. This leads to a hemispherical difference in properties of iron crystals, thereby creating the observed hemispherical dichotomy in seismic structure. Thus, the hemispheres in this case would result from a variation of effective inner core growth rate.

In our numerical tool, this model can be tested by considering effective growth rate as the proxy for seismic properties. This is synthesized as a very slow translation of the inner core, producing faster growth on one side than the other. The relationship between inner core growth rate and consequential iron properties is yet to be explored by mineral physicists. However, it is reasonable to assume that different growth rates result in variations of crystal properties, including size, shape, and orientation. Of course, such a difference may not be seismically detectable, or could be altered or even erased by subsequent events. Further mineral physics investigations are required here, for reconciliation with geodynamics and seismology.

To compute the effective growth rate for any point inside the sphere, we consider the value of the growth rate at the initial crystallization of that point, using the crystallization time and position. For the model of translation-rotation-growth, the effective growth rate is calculated at the inner core boundary as the combination of translation velocity and growth rate.

The growth rate results for slow translation are shown as a function of depth and longitude in Figure 4, as a random global data set and an equatorial contour plot. In the former, latitudinal variations introduce scatter into the values as a function of longitude, when projected onto the equator. We use this representation for easier comparison to WD11. Limiting the results to only those at the equator remove this problem (Figure 4, top). This also provides a method to estimate the dependence of growth rate on angular distance to the center of each hemisphere. Since these are estimated to be located on the equator, for data on the equator this corresponds simply to the difference in longitude between the two points.

We find that slow translation induces a hemispherical dichotomy in effective growth rate. This persists over the depth range explored, and has no noticeable lateral variation with depth. Thus, a slow translation is an appropriate approximation to a differential growth process, and is able to successfully generate the seismically-observed hemispherical difference.

The results for introducing superrotation to our slow translation model are shown in Figure 4. For the case of slow translation compared to fast, the addition of superrotation noticeably shifts the position of the boundaries with depth. The shift of the boundaries is asymmetric; the African boundary shifts 10°–20° more than the Pacific. This matches seismic observations (Waszek et al., 2011). For a translation velocity of about

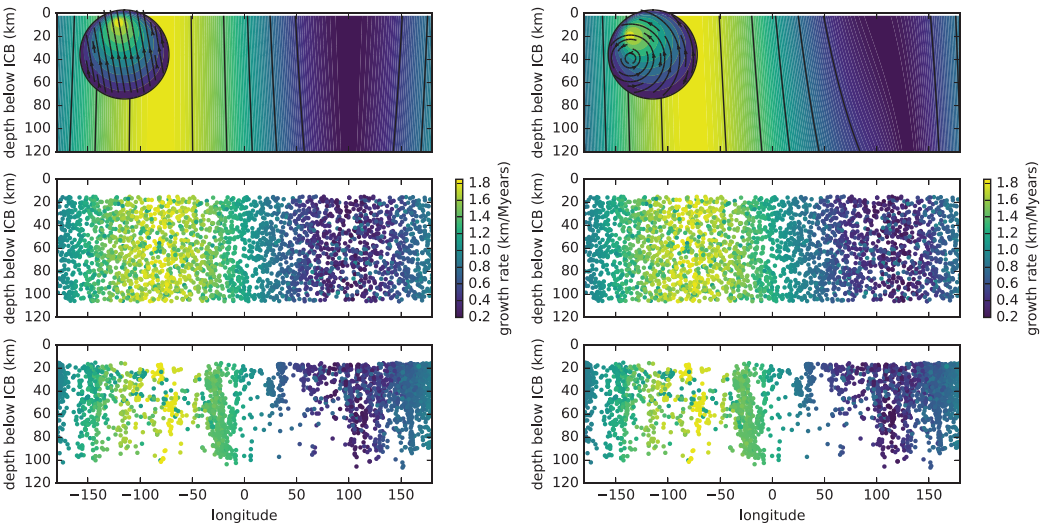

Figure 4. Value of the proxy (growth rate) as a function of the longitude and depth of the observation, for the slow translation model. Left column without rotation. Right column with rotation. As before in Figure 3, (top) contour maps are taken at the equator, and turning depths are from (middle) random global data set and (bottom) WD11.

0.98 km/Myr, the superrotation rate needed to shift one of the boundaries by 50 km of lateral movement over 100 km of depth is about 0.09°/Myr. This value is estimated based on the maximum shift observed in the iso-values on Figure 4 (top right) near the longitude 100°E.

The combination of slow translation and superrotation is the best candidate so far to explain the main characteristics of the hemisphere boundaries: possible sharpness, depth-shift of the hemisphere boundaries, and asymmetry. However, we have to point out some of the limitations of this model. Contrary to the fast translation, there is no published quantitative model to estimate seismic velocities and residuals from growth rate of iron crystals. Is it reasonable to qualitatively assume that different growing history could lead to different seismic properties, but there is no argument to justify that these differences would be seismically observable or not.

4. Conclusion

The seismic observations of the inner core are complex, with both large-scale and small-scale features. In this paper, we have been interested in the large-scale features of the uppermost inner core, namely the hemispherical dichotomy, and its variations with depth. We explored a particular subset of kinematic models for flow in the inner core where the velocity of material in the inner core is parametrized. For this models, we parametrized translation, rotation, and growth rate to explore the hemispherical dichotomy of the uppermost layer of the inner core. This is the first work to test directly the influence of a combination of inner core growth, translation, and superrotation, specifically applied to seismic properties.

Both fast and slow translations are able to generate an east-west asymmetry in age and growth rate respectively. However, the same rate of superrotation does not induce the same shift of properties in the deepest part of the isotropic layer. Previous studies (Geballe et al., 2013; Monnereau et al., 2010) already showed that the sharpness of the boundary can be explained by choosing one model to link age of material and seismic velocities. The fast and slow translations are thus not incompatible with the sharp hemispherical boundary. The observations of a shift in depth of the boundary position have raised the possibility of a slow superrotation of the inner core. Our results show that even if such a superrotation could be coupled with the fast translation proposed by Monnereau et al. (2010) and Alboussière et al. (2010), this would not lead to the observed shift in depth, but only to a difference between the African and Pacific boundaries. Furthermore, we also showed that for a slow translation, adding superrotation would indeed induce both the asymmetry of the boundary and a noticeable shift with depth. It is however important to note that no mechanism to drive the superrotation is proposed here. Further study is needed in order to drive at the same time a superrotation and a slow translation.

We explored the validity of using a real seismic data, by comparing WD11 with a random data set, with the same number of raypaths which are homogeneously distributed in the uppermost inner core. This is the first use of a real data set to sample geodynamic models. From this, we are able to infer that the real data set is certainly sufficient to characterize the large-scale heterogeneities of the layer. Our models are also able to introduce smaller scale variation into the proxies, including asymmetry in both hemisphere size and boundary sharpness; these correspond to seismic observations. However, the data coverage as a function of depth is sparse at the boundaries between the two hemispheres, and complex structure near the boundary is therefore poorly constrained with this data set. Additional seismic data is required in these regions.

We have also presented a new open-source Python code GrowYourIC, which synthesizes growth, translation, and superrotation of the inner core. The code generates age, age gradient, and growth rate models for the inner core, and calculates averages parameters along inner core raypaths. The paths may be random or user specified, and we include a real inner core data set from Waszek and Deuss (2011), WD11, as an example. As supporting information, we have provided all of the necessary information for the reader to recreate results presented here, as well as develop additional functions. The tool is highly modular, allowing users to add models for geodynamics and seismic data set.

We hope this is a first step toward developing user-friendly, open-access tools for combining seismic and geodynamic studies, and that it will encourage other researchers to share their own codes, materials, and data. The ability to compare several data sets, or results from various geodynamic models, will be the next stage for this project.

There are many future directions for this project. A major next step is to incorporate mineral physics models, in order to provide realistic conversions from age and growth rate to seismic properties such as velocity and attenuation. Further possibilities include mechanisms to create anisotropy, and the introduction of differences in composition, for example between the hemispheres, or with depth. Our results show the importance of a multidisciplinary approach for understanding the processes of the inner core, and for orienting future research questions.

Appendix A: Code Operation

GrowYourIC is a Python tool available freely online. The version used to perform the calculations in this paper is version 0.2. This version as well as the most up-to-date version is available at https://github.com/MarineLasbleis/GrowYourIC.

To operate the code, the user provides information regarding seismic distribution and raypaths of the PKIKP through the inner core. The user also provides either parameters for the included kinematic models (see below) or velocity fields for external models. The toolbox calculates proxies and provides visualization tools. The visualization tools may also be used without seismic data sets, to visualize the model only and constructing heat maps on various contours or slices.

The input seismic data sets are a set of PKIKP raypaths in the inner core, defined by three points: entry, turning, and exit. Real paths have an associated travel time residual measurement which is provided. For each data point on the trajectory, the code calculates a proxy value. This can be averaged over the raypath, either linearly or via the average of the proxy's inverse. In this paper, we present results obtained only at the turning bottom point, for comparison with the analysis performed in WD11.

An overview of the different possible output graphs is given in supporting information Figures S3 and S4. All the figures in this manuscript—including supporting information—are implemented as Jupyter Notebooks (Kluyver et al., 2016) and available online.

A1. Implemented Geodynamical Models

The toolbox GrowYourIC can handle various geodynamic models, the only requisites being either the proxy field already calculated from the model or the knowledge of velocity flow in the inner core for its entire history and volume. For this paper, we apply the code to a basic analytical version of translation and rotation. However, velocity fields can be computed from most published geodynamic models, to permit further models to be included in future.

Flow models for the inner core have already been implemented in GrowYourIC: any combination of translation, superrotation, and growth is permissible, including time-variations in the velocities. They are defined by imposing a velocity field in the inner core, and thus are kinematic models. Each model is defined by a velocity field $v(\mathbf{r}, t)$, which is input as an analytical function. The values used in this paper have been chosen based on published estimates of the translation velocity for fast and slow translation (Alboussière et al., 2010; Aubert et al., 2008), growth rate (Labrosse, 2003), and reasonable values of superrotation based on observations (Waszek et al., 2011). To simplify the models presented here, we consider only constant values of the velocities, and a growth history as $r_{icb}(t) \propto t^{\alpha}$, where t is the time after the first nucleus. The models presented in this publication are summarized in Figure 1a, and the corresponding parameters values are given in the supporting information. Static models, such as those based on the geometry of the inner core, are also implemented. These can be used for simple hemispherical models, for example, or user-defined crystal orientation.

Users can provide external models to GrowYourIC directly. The only requisite is to provide a field-type proxy, which is defined for a given model as a function $proxy = g(\mathbf{r})$. A velocity field $v(\mathbf{r}, t)$ can also be provided, and GrowYourIC calculates material trajectory, age, etc. based on the velocity field.

A2. Proxies

For each point of interest, the code extracts the value of *proxies*. These proxies are considered to reflect the current seismic properties of the material. This includes for example: position at crystallization, age (time since crystallization), and growth rate at crystallization time. When material is not deformed, the variation in seismic velocities is likely to be controlled by crystal size, which depend either on the initial conditions, i.e., growth rate at crystal formation, or on the age and evolution of the crystal, or a combination of all.

Kinematic models include velocity fields and are the ones of interest in this paper. Each point in the inner core is associated with a flow line, which is the trajectory of the material since its first crystallization. The intersection of this trajectory with the inner core boundary is calculated to obtain the position and time of the crystallization of this point. To do so, we integrate the velocity field backward using the Runge-Kutta integration method. This trajectory is used to calculate average values over time.

The code includes the option to add the function f relating mineral and seismic properties to proxies. For the interested user, modules for the GE13 mineral models have been implemented in the toolbox; we do not duplicate the results of that previous work here.

A3. Representations and Available Databases

The toolbox GrowYourIC provides databases of points where to evaluate proxy values. Two types of database are available, either to visualize the model or to use seismic data.

The databases constructed for visualization purpose are perfect sampling of the part of the inner core that need to be visualized. Proxy values are evaluated only at the given positions, and not over a raypath. These databases allow the creation of a heat map of the proxy in a certain geometry. Examples are the databases used for visualization in Figure 1a, and in the top of Figures 2 and 4. Visualization routines are directly implemented within the definition of the database.

The other type of databases are constructed with raypaths of PKIKP through the inner core; either user-specified raypaths, or random distribution used to mimic a real seismic data set. Each inner core raypath is determined by providing three points: entry, turning, and exit. Entry and exit points are by definition at the surface of the inner core.

Acknowledgments

M.L. was funded by International Research Fellowship of the Japan Society for the Promotion of Science. L.W. is the recipient of a Discovery Early Career Research Award (project DE170100329) funded by the Australian Research Concil. At Cambridge, L.W. was funded by a Junior Research Fellowship from Homerton College, and E.D. was funded by the European Research Council under the European Community's Seventh Framework Programme (FP7/2007–2013)/ERC grant 204995. This project initially started during the CIDER 2012 Summer School. CIDER-II is funded as a "Synthesis Center" by the Frontiers of Earth Systems Dynamics (FESD) program of NSF under grant EAR-1135452. We thank David Al-Attar for insight and discussion. We also thank the Editor, Thorsten Becker, and Satoru Tanaka for helpful review and comments that improved the manuscript. Figures and results in this manuscript have been generated with version 0.2 of the package. This version as well as the most up-to-date version is available at https://github.com/MarineLasbleis/GrowYourIC.

References

Alboussière, T., Deguen, R., & Melzani, M. (2010). Melting-induced stratification above the Earth's inner core due to convective translation. *Nature*, *466*, 744–747.

Aubert, J., Amit, H., Hulot, G., & Olson, P. (2008). Thermochemical flows couple the Earth's inner core growth to mantle heterogeneity. *Nature*, *454*, 758–762.

Aubert, J., & Dumberry, M. (2011). Steady and fluctuating inner core rotation in numerical geodynamo models. *Geophysical Journal International*, *184*, 162–170.

Aubert, J., Finlay, C. C., & Fournier, A. (2013). Bottom-up control of geomagnetic secular variation by the Earth's inner core. *Nature*, *502*(7470), 219–223.

Bergman, M., Lewis, D., Myint, I., Slivka, L., Karato, S., & Abreu, A. (2010). Grain growth and loss of texture during annealing of alloys, and the translation of Earth's inner core. *Geophysical Research Letters*, *37*, L22313. https://doi.org/10.1029/2010GL045103

Calvet, M., & Margerin, L. (2008). Constraints on grain size and stable iron phases in the uppermost inner core from multiple scattering modeling of seismic velocity and attenuation. *Earth and Planetary Science Letters*, *267*, 200–212.

Cao, A., & Romanowicz, B. (2004). Hemispherical transition of seismic attenuation at the top of the Earth's inner core. *Earth and Planetary Science Letters*, *228*(3–4), 243–253.

Cormier, V., Attanayake, J., & He, K. (2011). Inner core freezing and melting: Constraints from seismic body waves. *Physics of the Earth and Planetary Interiors*, *188*, 163–172.

Creager, K. (1992). Anisotropy of the inner core from differential travel times of the phases PKP and PKIKP. *Nature*, *356*, 309–314.

Creager, K. (2000). Inner core anisotropy and rotation. In *Earth's deep interior: Mineral physics and tomography from the atomic to the global scale, geophysical monograph* (Vol. 117, pp. 89–114). Washington, DC: American Geophysical Union.

Deguen, R., Alboussière, T., & Cardin, P. (2013). Thermal convection in Earth's inner core with phase change at its boundary. *Geophysical Journal International*, *194*(3), 1310–1334.

Deguen, R., Cardin, P., Merkel, S., & Lebensohn, R. (2011). Texturing in Earth's inner core due to preferential growth in its equatorial belt. *Physics of the Earth and Planetary Interiors*, *188*, 173–184.

Deuss, A., Irving, J., & Woodhouse, J. (2010). Regional variation of inner core anisotropy from seismic normal mode observations. *Science*, *328*, 1018–1020.

Garcia, R., & Souriau, A. (2000). Inner core anisotropy and heterogeneity level. *Geophysical Research Letters*, *27*, 3121–3124.

Geballe, Z. M., Lasbleis, M., Cormier, V. F., & Day, E. A. (2013). Sharp hemisphere boundaries in a translating inner core. *Geophysical Research Letters*, *40*, 1719–1723. https://doi.org/10.1002/grl.50372

Gubbins, D., Alfe, D., & Davies, C. (2013). Compositional instability of earth's solid inner core. *Geophysical Research Letters*, *40*, 1084–1088. https://doi.org/10.1002/grl.50186

Irving, J. (2016). Imaging the inner core under Africa and Europe. *Physics of the Earth and Planetary Interiors*, *254*, 12–24.

Irving, J., & Deuss, A. (2011a). Hemispherical structure in inner core velocity anisotropy. *Journal of Geophysical Research*, *16*, B04307. https://doi.org/10.1029/2010JB007942

Irving, J., & Deuss, A. (2011b). Stratified anisotropic structure at the top of Earth's inner core: A normal mode study. *Physics of the Earth and Planetary Interiors*, *186*, 59–69.

Irving, J., & Deuss, A. (2015). Regional seismic variations in the inner core under the North Pacific. *Geophysical Supplements to the Monthly Notices of the Royal Astronomical Society*, *203*(3), 2189–2199.

Kluyver, T., Ragan-Kelley, B., Pérez, F., Granger, B., Bussonnier, M., Frederic, J., . . . Jupyter Development Team. (2016). Jupyter Notebooks—A publishing format for reproducible computational workflows. In *ELPUB* (pp. 87–90).

Labrosse, S. (2003). Thermal and magnetic evolution of the Earth's core. *Physics of the Earth and Planetary Interiors*, *140*, 127–143.
Lasbleis, M., & Deguen, R. (2015). Building a regime diagram for the Earths inner core. *Physics of the Earth and Planetary Interiors*, *247*, 80–93.
Lincot, A., Cardin, P., Deguen, R., & Merkel, S. (2016). Multiscale model of global inner-core anisotropy induced by hcp alloy plasticity. *Geophysical Research Letters*, *43*, 1084–1091. https://doi.org/10.1002/2015GL067019
Lincot, A., Deguen, R., Merkel, S., & Cardin, P. (2014). Seismic response and anisotropy of a model hcp iron inner core. *Comptes Rendus Geoscience*, *346*(5–6), 148–157.
Lincot, A., Merkel, S., & Cardin, P. (2015). Is inner core seismic anisotropy a marker for plastic flow of cubic iron? *Geophysical Research Letters*, *42*, 1326–1333. https://doi.org/10.1002/2014GL062862
Lythgoe, K. H., Deuss, A., Rudge, J. F., & Neufeld, J. A. (2014). Earth's inner core: Innermost inner core or hemispherical variations? *Earth and Planetary Science Letters*, *385*(C), 181–189.
Lythgoe, K. H., Rudge, J. F., Neufeld, J. A., & Deuss, A. (2015). The feasibility of thermal and compositional convection in Earth's inner core. *Geophysical Journal International*, *201*(2), 764–782.
Miller, M. S., Niu, F., & Vanacore, E. A. (2013). Aspherical structural heterogeneity within the uppermost inner core: Insights into the hemispherical boundaries and core formation. *Physics of the Earth and Planetary Interiors*, *223*, 8–20.
Mizzon, H., & Monnereau, M. (2013). Implication of the lopsided growth for the viscosity of Earth's inner core. *Earth and Planetary Science Letters*, *361*, 391–401.
Monnereau, M., Calvet, M., Margerin, L., & Souriau, A. (2010). Lopsided growth of Earth's inner core. *Science*, *328*, 1014–1017.
Morelli, A., Dziewoński, A., & Woodhouse, J. (1986). Anisotropy of the inner core inferred from PKIKP travel times. *Geophysical Research Letters*, *13*, 1545–1548.
Niu, F., & Wen, L. (2001). Hemispherical variations in seismic velocity at the top of the Earth's inner core. *Nature*, *410*, 1081–1084.
Niu, F., & Wen, L. (2002). Seismic anisotropy in the top 400 km of the inner core beneath the "eastern" hemisphere. *Geophysical Research Letters*, *29*(12), https://doi.org/10.1029/2001GL014118
Ouzounis, A., & Creager, K. (2001). Isotropy overlying anisotropy at the top of the inner core. *Geophysical Research Letters*, *28*, 4331–4334.
Poupinet, G., Pillet, R., & Souriau, A. (1983). Possible heterogeneity of the Earth's core deduced from PKIKP travel times. *Nature*, *305*, 204–206.
Shearer, P. (1994). Constraints on inner core anisotropy from PKP(DF) travel times. *Journal of Geophysical Research*, *99*, 19647–19659.
Song, X., & Helmberger, D. (1995). Depth dependence of anisotropy of Earth' inner core. *Journal of Geophysical Research*, *100*, 9805–9816.
Song, X., & Richards, P. (1996). Seismological evidence for differential rotation of the Earth's inner core. *Nature*, *382*, 221–224.
Song, X., & Xu, X. (2002). Inner core transition zone and anomalous PKP(DF) waveforms from polar paths. *Geophysical Research Letters*, *29*(4). https://doi.org/10.1029/2001GL013822
Souriau, A. (2009). Inner core structure: Constraints from frequency dependent seismic anisotropy. *Comptes Rendus Geoscience*, *341*, 439–445.
Souriau, A., & Romanowicz, B. (1996). Anisotropy in inner core attenuation: A new type of data to constrain the nature of the solid core. *Geophysical Research Letters*, *23*, 1–4.
Tanaka, S., & Hamaguchi, H. (1997). Degree one heterogeneity and hemispherical variation of anisotropy in the inner core from *PKP*(BC)–*PKP*(DF) times. *Journal of Geophysical Research*, *102*, 2925–2938.
Vidale, J., & Earle, P. (2000). Fine-scale heterogeneity in the Earth's inner core. *Nature*, *404*, 273–275.
Waszek, L., & Deuss, A. (2011). Distinct layering in the hemispherical seismic velocity structure of Earth's upper inner core. *Journal of Geophysical Research*, *116*, B12313. https://doi.org/10.1029/2011JB008650
Waszek, L., Irving, J., & Deuss, A. (2011). Reconciling the hemispherical structure of Earth's inner core with its super-rotation. *Nature Geoscience*, *4*, 264–267.
Woodhouse, J., Giardini, D., & Li, X. (1986). Evidence for inner core anisotropy from free oscillations. *Geophysical Research Letters*, *13*, 1549–1552.
Yoshida, S., Sumita, I., & Kumazawa, M. (1996). Growth model of the inner core coupled with the outer core dynamics and the resulting elastic anisotropy. *Journal of Geophysical Research*, *101*, 28085–28103.
Yu, W., & Wen, L. (2007). Complex seismic anisotropy in the top of the Earth's inner core beneath Africa. *Journal of Geophysical Research*, *112*, B08304. https://doi.org/10.1029/2006JB004868